Heterogeneous Uptake of 8−2 Fluorotelomer Alcohol on Liquid Water and 1-Octanol Droplets†

Yongquan Li and Kenneth L. Demerjian

Atmospheric Sciences Research Center, State University of New York, 251 Fuller Road, Albany, New York 12203

Leah R. Williams,* Douglas R. Worsnop, and Charles E. Kolb

Center for Cloud and Aerosol Chemistry, Aerodyne Research, Inc., 45 Manning Road, Billerica, Massachusetts 01821-3976

Paul Davidovits

Chemistry Department, Boston College, Chestnut Hill, Massachusetts 02467-3809

Received: November 1, 2005; In Final Form: January 24, 2006

The heterogeneous uptake of the 8−2 fluorotelomer alcohol, $F(CF_2)_8CH_2CH_2OH$, on liquid water surfaces over the temperature range 256−273 K and on 1-octanol surfaces over the temperature range 264−295 K has been investigated with a droplet train flow reactor. The uptake coefficient on water droplets is zero within the error of the measurement (±0.01) and is independent of droplet temperature. In contrast, significant uptake onto 1-octanol is observed. Measured uptake coefficients for 1-octanol showed a negative temperature dependence, varying from 0.034 ± 0.005 (1σ) at 295 K to 0.103 ± 0.009 at 264 K. The measured uptake coefficients on 1-octanol were independent of gas−liquid contact time, for typical contact times varying between 3 and 15 ms, and independent of the 8−2 fluorotelomer alcohol gas-phase concentration, indicating that the uptake coefficients are equivalent to mass accommodation coefficients. The uptake coefficients on 1-octanol were also independent of relative humidity. These results show that the uptake of FTOHs on or into the aqueous component of cloud/fog droplets or aqueous aerosol particles is not likely to be an important atmospheric sink for these compounds. In these experiments, 1-octanol was used as a model compound for organic-containing atmospheric particles. The larger uptake coefficient measured for 1-octanol surfaces indicates that FTOH partitioning to organic-containing cloud/fog droplets and aerosol particles may be an atmospheric loss mechanism.

Introduction

Fluorotelomer alcohols (FTOHs) are polyfluorinated linear molecules with the formula $F(CF_2)_nCH_2CH_2OH$ and are typically designated n−2 FTOH where n is the number of fluorinated carbons (n = 6, 8, 10, and 12 are most common). FTOHs are used as a raw material in the manufacture of fluorotelomer-based surfactant and polymeric products that provide surface modification properties in a wide variety of end uses.[1,2] The surface-active nature of fluorotelomer-based products originates from the rigid, hydro-, and oleophobic fluorotelomer functionality. FTOHs are a residual raw material present in products and have sufficient vapor pressure to be present in the gas phase.[3,4] Residual FTOH materials are likely to be released to air during industrial use.[5] The 6−2, 8−2, and 10−2 FTOHs have been detected in the atmosphere over several North American sites in concentrations ranging from 11 to 165 pg m^{-3}.[6,7] FTOHs are of interest because their gas-phase atmospheric oxidation may produce perfluorinated carboxylic acids,[8−10] which are known to be highly persistent environmental pollutants.[11]

The gas-phase oxidation chemistry of FTOH compounds has been studied by several groups. FTOHs have been shown to react with photochemically produced hydroxyl radicals to produce the corresponding fluorotelomer aldehydes $CF_3(CF_2)_n$-CH_2CHO as sole primary oxidation products.[9] This initial oxidation reaction has been well-studied and yields a relatively short atmospheric FTOH chemical lifetime of ∼10−20 days. The fluorotelomer aldehydes can in turn be oxidized to produce perfluorinated aldehydes $CF_3(CF_2)_nCHO$ as secondary oxidation products. Smog chamber studies indicate that perfluorinated carboxylic acids may be produced as one of several tertiary oxidation products under low NO_x conditions, although there is considerable uncertainty about the chemical mechanisms involved and the yield of perfluorinated carboxylic acids. Under conditions with high ambient [NO] + [NO_2], the fluorotelomer alcohols will oxidize to produce fluorinated aldehydes and organic nitrates with little predicted formation of perfluorocarboxylic acids.[8,12]

FTOHs may also be removed from the atmosphere by mechanisms other than homogeneous chemistry. Experimental and theoretical studies have ruled out direct photolysis of FTOHs,[13] and wet deposition is limited by the low aqueous solubilities of the FTOHs.[4,14]

† Part of the special issue "David M. Golden Festschrift".

* Corresponding author. Phone: 978-663-9500 x421. Fax: 978-663-4918. E-mail: Williams@aerodyne.com.

10.1021/jp0563134 CCC: $33.50
Published on Web 03/29/2006

In contrast to the extensive work on gas-phase reactivity, there has been little study of the atmospheric heterogeneous fate of FTOHs. Estimates of aqueous Henry's law constants would suggest that significant heterogeneous uptake by aqueous cloud and aerosol droplets in the traditional sense of mass accommodation followed by aqueous-phase solvation or reaction is unlikely. However, there remains a possibility that the fluorotelomer alcohols will condense on the surface of aqueous droplets and either remain dispersed on the surface acting as a surfactant or segregate into a separate organic phase. It is worth noting that both effects have previously been advanced to explain observations that a range of high molecular weight organic species, including pesticides and plasticizers, are found to be enriched in fog droplets at ratios up to several thousand times higher than their aqueous Henry's law constants would allow.[15,16]

If the FTOH compounds showed a propensity to condense on or dissolve in atmospheric cloud droplets and/or aerosol particles, this atmospheric lifetime could be shortened significantly. To date, there has been no comprehensive study of the heterogeneous uptake of gas-phase FTOHs on liquid droplets, and the effect of uptake on atmospheric lifetime is unknown.

In this paper, we report temperature-dependent droplet train flow reactor studies of the heterogeneous uptake kinetics of gas-phase 8−2 fluorotelomer alcohol ($F(CF_2)_8CH_2CH_2OH$, 8−2 FTOH) on liquid water surfaces, representing cloud droplets and deliquescent aerosol particles, and on 1-octanol surfaces, chosen as a model for atmospheric organic particles based on the use of octanol−air partition coefficients to model gas to particle partitioning.[17,18] We have also performed the 1-octanol studies as a function of relative humidity to see if the presence of water vapor affects uptake on organic surfaces.

Gas−Liquid Interactions

In the droplet train flow reactor, a gas-phase species interacts with a continuously renewed stream of liquid droplets, and the disappearance of the species from the gas-phase is monitored. The measured loss of gas-phase molecules can be interpreted in terms of a phenomenological description of gas−liquid interactions. First, the gas-phase molecule is transported to the liquid surface, usually by gas-phase diffusion. The subsequent entry of the species into the liquid is governed by the mass accommodation coefficient, α, which is the probability that a molecule striking a liquid surface enters into the bulk liquid phase. Mass accommodation can be thought of as a two-step process involving surface adsorption followed by a competition between desorption and solvation.[19] Other possible steps in the gas−liquid interaction include reaction at the surface, reaction in the bulk liquid, and diffusion back to the surface followed by re-evaporation. Each of these steps can be probed by varying the conditions of the droplet train flow reactor experiment.

In the absence of surface reactions, the mass accommodation coefficient limits the maximum flux, J (molecules cm^{-2} s^{-1}), of gas into a liquid

$$J = \frac{n_g \bar{c} \alpha}{4} \tag{1}$$

Here, n_g (molecules cm^{-3}) is the molecular density of the gas molecules, and $\bar{c}$ (cm s^{-1}) is the average thermal speed. If reactions occur at the gas−liquid interface, then the flux of species disappearing from the gas phase may exceed that given by eq 1. The flux cannot exceed the collision rate of $(n_g\bar{c})/4$.

Two additional effects limit the net flux. First, as the gas molecules enter the liquid, new molecules have to move toward the liquid surface to replenish the gas-depleted region near the liquid surface. The rate of transport toward the liquid surface is determined by gas-phase diffusion that can limit the rate of uptake by the liquid. Second, as the gas-phase species enters the bulk liquid, a fraction evaporates back into the gas phase. This process is governed by gas/liquid partitioning. The experimentally observed flux (J_{meas}) into a surface may be expressed in terms of a measured uptake coefficient, γ_{meas}, that takes into account these effects.

$$J_{means} = \frac{n_g \bar{c} \gamma_{meas}}{4} \tag{2}$$

To a good approximation, these effects can be de-coupled, and γ_{meas} can be expressed as the sum of the gas-phase diffusion resistance and the uptake coefficient, γ_0, due to gas−liquid interactions in the limit of "zero pressure", i.e., under conditions where gas-phase diffusion does not limit the flux across the interface

$$\frac{1}{\gamma_{meas}} = \frac{1}{\Gamma_{diff}} + \frac{1}{\gamma_0} \tag{3}$$

The parameter Γ_{diff} takes into account the effect of gas-phase diffusion on the uptake. In this formulation, n_g is the density of the gas-phase species far from the droplet train. The gradient in the gas density due to depletion near the droplet surface is taken into account by Γ_{diff}. Analytical equations for gas-phase diffusive transport of a trace gas to a train of moving droplets do not exist. However, an empirical formulation of diffusive transport to a stationary droplet developed by Fuchs and Sutugin[20] has been shown to be in good agreement with measurements[21,22] and can be modified for use with a train of moving droplets. In the Fuchs−Sutugin formulation, Γ_{diff} for a single droplet is expressed as[23]

$$\frac{1}{\Gamma_{diff}} = \frac{0.75 + 0.283\mathrm{Kn}}{\mathrm{Kn}(1 + \mathrm{Kn})} \tag{4}$$

where the Knudsen number $\mathrm{Kn} = 2\lambda/d_f$, λ (cm) $= 3D_g/\bar{c}$ is the gas-phase mean free path, d_f (cm) is the droplet diameter, and D_g (cm^2 s^{-1}) is the gas-phase diffusion coefficient. In a train of moving droplets, the Fuchs−Sutugin expression is modified by setting

$$\mathrm{Kn} = \lambda/d_0 \tag{5}$$

where d_0 (cm) is the diameter of the droplet forming orifice. Note that the effective Knudsen number defined by eq 5 for calculating the gas-phase diffusion correction in the droplet train experiments depends on the orifice diameter and not on the diameter of the droplets. Equation 5 for the effective Knudsen number was determined empirically from droplet train flow reactor experiments over a wide range of Knudsen numbers, gas mixtures, and uptake coefficients.[24] Recent theoretical calculations of gas-phase diffusion in a droplet train flow reactor by Morita et al.[25] support the conclusion that the effective Knudsen number depends on the orifice diameter rather than the droplet diameter.

The parameter γ_0 accounts for the effects on the gas uptake of the mass accommodation coefficient, Henry's law solubility, and liquid-phase or surface reactions, if any. In the absence of chemical reactions, a simple approximate expression for γ_0 is

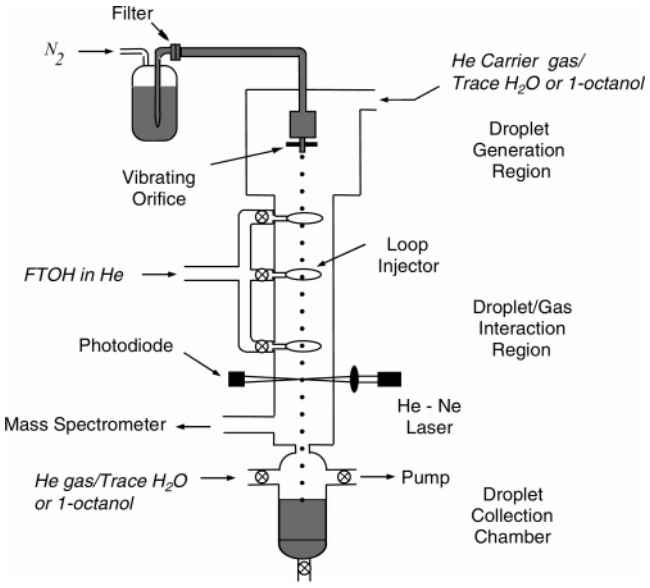

Figure 1. Schematic of the droplet train flow reactor.

obtained by decoupling the mass accommodation, α, and solubility limitation processes

$$\frac{1}{\gamma_0} = \frac{1}{\alpha} + \frac{1}{\Gamma_{sat}} \tag{6}$$

The term Γ_{sat} takes into account re-evaporation of trace gas molecules that have entered the bulk liquid phase (i.e., Γ_{sat} represents the effect of gas/liquid partitioning). Γ_{sat} can be approximated by the expression[26,27]

$$\frac{1}{\Gamma_{sat}} = \frac{\bar{c}}{8RTH}\sqrt{\frac{\pi t}{D_1}} \tag{7}$$

Here, D_l (cm^2 s^{-1}) is the liquid-phase diffusion coefficient of the trace gas species in the droplet, t (s) is the gas−liquid interaction time, R (L atm K^{-1} mol^{-1}) is the gas constant, T (K) is the gas-phase temperature, and H (M atm^{-1}) is the Henry's law constant. Note that Γ_{sat} measures the extent to which the gas-phase species is out of equilibrium with the liquid. As equilibrium is approached, Γ_{sat} approaches 0.

Experimental Description

In the droplet train flow reactor shown in Figure 1,[26,28] heterogeneous uptake is measured by exposing a trace gas species to a fast-moving, monodisperse, spatially collimated train of liquid droplets. The droplet train is produced by forcing the liquid, distilled water or 1-octanol in these experiments, through a 70-μm-diameter platinum electron microscope aperture surrounded by a donut-shaped piezoelectric ceramic. For a given liquid flow rate (typically 10^{-7} m^3 s^{-1}), the number of droplets produced per second and their diameter are determined by the driving frequency applied to the piezoelectric ceramic. The driving frequency was switched between around 3 kHz and around 30 kHz, generating droplets with diameters of 3.0×10^{-4} m and 2.0×10^{-4} m, respectively. The liquid was cooled to the desired temperature before entering the vibrating orifice.

The droplet train passes through a 30-cm-long, 1.4-cm-inner-diameter, longitudinal low-pressure (3.5−15 Torr or 467−2000 Pa) flow reactor that contains the trace gas species, in this case, 8−2 FTOH, at a concentration of approximately 2×10^{14} molecules cm^{-3}. The trace gas is entrained in a carrier gas mixture consisting of an inert gas (usually helium) and water or 1-octanol vapor at a partial pressure in equilibrium with the liquid droplets. Careful matching of the water or 1-octanol vapor with the equilibrium vapor pressure of the droplets ensures that condensation or evaporation does not change the temperature or size of the droplets.

The trace gas is introduced through one of three loop injectors located along the flow tube. By selecting the gas inlet port and the droplet velocity, the gas−droplet interaction time can be varied between about 3 and 15 ms. The flow tube wall is heated to 323 K to prevent condensation on the walls and thus improve the stability of the experiment.

The velocity of the liquid droplets is determined by the orifice diameter and the pressure of the gas that forces the liquid through the orifice and is in the range 1.2−3.0 m s^{-1}. The uniformity of the droplets and the droplet velocity along the flow tube are monitored by passing cylindrically focused He−Ne laser beams through the droplet train at three heights along the flow tube (only one laser beam is shown in Figure 1).[28] The droplet velocity along the flow tube is measured to be constant to within 3%. Note that these droplets are large enough ($>2.0 \times 10^{-4}$ m in diameter) that their curvature has a negligible effect on the equilibrium vapor pressure.

Uptake coefficients are measured by switching the droplet generating frequency and thus the surface area of the droplets. A measured decrease in the trace gas concentration resulting from an increase in the exposed droplet surface area corresponds to uptake of the gas by the increased droplet surface area. The density of the trace gas is monitored with a quadrupole mass spectrometer. The 8−2 fluorotelomer alcohol concentration was monitored at m/z 95, corresponding to the $C_3F_3H_2^+$ fragment ion.

The uptake coefficient (γ_{meas}) as defined by eq 2 is calculated from the measured change in trace gas signal via eq 8[19,28]

$$\gamma_{meas} = \frac{4F_g}{\bar{c}\Delta A} \ln \frac{n_g}{n_g'} \tag{8}$$

Here, F_g (cm^3 s^{-1}) is the carrier-gas volume flow rate (∼100 to 500 cm^3 s^{-1}) through the system, ΔA (cm^2) $= A_1 - A_2$ is the change in the total droplet surface area in contact with the trace gas, and n_g (molecules cm^{-3}) and n_g' (molecules cm^{-3}) are the trace gas densities at the outlet of the flow tube after exposure to droplets of areas A_2 and A_1, respectively.

To minimize the effect of gas-phase diffusion, uptake is usually measured at the lowest possible overall gas pressure in the flow tube. The minimum operating pressure for this experiment was 3.5 Torr (467 Pa), where the operating pressure is the sum of the partial pressures of the carrier gas, the added vapor corresponding to the equilibrium vapor pressure of the droplets, and the trace gas. The added 1-octanol vapor pressure ranged from 0.016 Torr (2.1 Pa) at 264 K to 0.21 Torr (28 Pa) at 295 K. For the water droplet experiments, the added water vapor ranged from 1.4 Torr (187 Pa) at 257 K to 4.6 Torr (613 Pa) at 273 K. The partial pressure of the 8−2 FTOH in the flow tube was typically 0.008 Torr (1 Pa or about 3×10^{14} molecules cm^{-3}) after dilution by the carrier gases. Experiments were also conducted as a function of Knudsen number, Kn, by increasing the partial pressure of the He carrier gas or by using Ar as the carrier gas.

The overall pressure balance in the flow tube was checked by monitoring simultaneously both the trace species studied and the concentration of an inert reference trace gas, in this case, Xe, that is effectively insoluble in the liquid droplets. Any change in the reference gas concentration with droplet switching

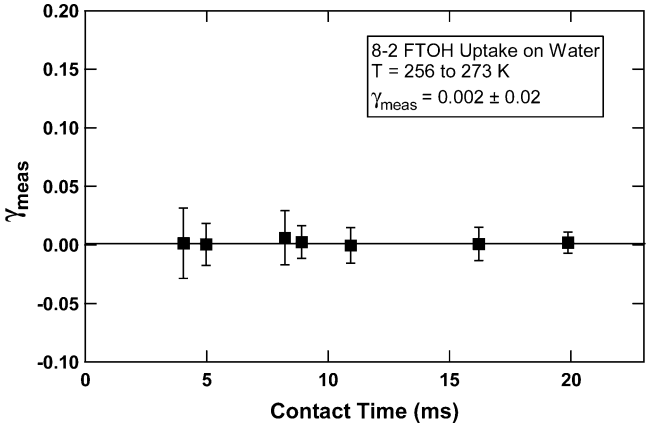

Figure 2. Measured uptake coefficient for 8−2 FTOH on water as a function of gas−droplet contact time. Data at four different droplet temperatures are averaged together.

determines the "zero" of the system and was subtracted from observed changes in trace gas concentration. In the present experiments, this correction was less than 5%.

We tested for wall loss by turning off the droplet generation system and injecting the 8−2 FTOH through each of the three loop injectors. If 8−2 FTOH is lost to the walls of the flow tube, this would be evident as a decrease in 8−2 FTOH concentration with increasing exposure time to the walls. No change in the 8−2 FTOH concentration was observed. Therefore, wall loss in this experiment is negligible, and no correction for wall loss has been applied to the measured uptake coefficients.

The 8−2 FTOH was obtained from E. I. du Pont de Nemours Co. (Wilmington, DE) and used as provided. The 1-octanol (reagent grade) was obtained from Aldrich (Milwaukee, WI) and used without further purification. The water was treated with a Millipore (Billerica, MA) filter system (Milli-DI, >1 MΩ cm) before use.

Results and Analysis

Uptake on Water Droplets. Figure 2 shows the measured uptake coefficient for 8−2 FTOH on water as a function of gas−droplet contact time. The uptake coefficient is zero within the error of the measurement (±0.01 at contact times >10 ms) and is independent of droplet temperature. Data collected at four different droplet temperatures between 256 and 273 K are averaged together in Figure 2. The concentration of 8−2 FTOH was varied over 1 order of magnitude with no effect on the uptake coefficient. The error bars are derived from multiple measurements (at least three) under the same conditions. Note that the error bars are larger at shorter contact times, because it takes some time for laminar flow to redevelop after the trace gas is injected through the loop injector into the carrier gas flow. At the shortest contact times, the flow disruption introduces a larger, random error into the gas−droplet contact conditions.

Uptake on 1-Octanol Droplets. Figure 3 shows typical experimental data for the uptake of 8−2 FTOH on 1-octanol droplets at 268 K plotted as $\ln(n_g/n'_g)$ vs $\bar{c}\Delta A/4F_g$. The value of $\bar{c}\Delta A/4F_g$ was changed by varying the gas flow rate. Each point in Figure 3 is an average over ten changes in surface area, and the error bars represent one standard deviation in $\ln(n_g/n'_g)$. The slope of the least-squares fit through the points gives γ_{meas} as shown in eq 8. For this set of data, $\gamma_{meas} = 0.075 \pm 0.003$, where the error bar is derived from the least-squares fit and the error on each point. The intercept (0.0005 ± 0.003) is slightly nonzero but is within the error bar of zero, indicating no

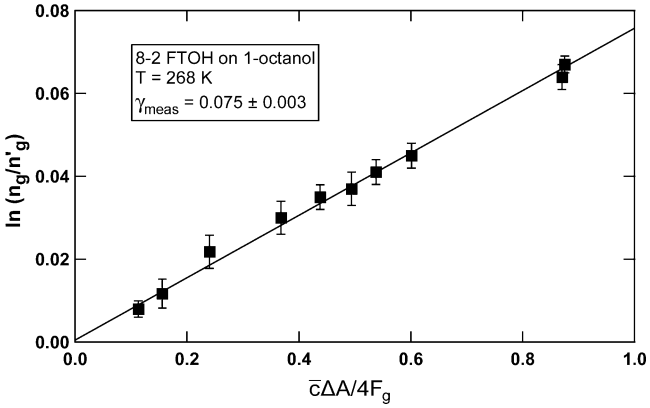

Figure 3. Plot of $\ln(n_g/n'_g)$ vs $\bar{c}\Delta A/4F_g$ for 8−2 FTOH uptake on 1-octanol droplets at 268 K. Solid line is the least-squares fit to the data. Slope of the solid line is $\gamma_{meas} = 0.075 \pm 0.003$ (see eq 8).

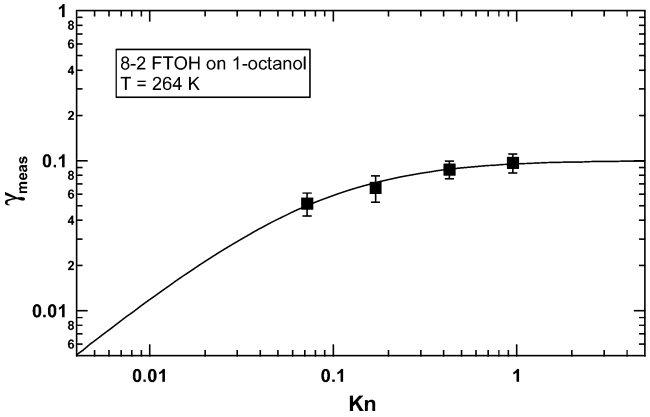

Figure 4. Uptake coefficient, γ_{meas}, as a function of Kn for FTOH uptake on 1-octanol droplets at 264 K. The line is calculated from eq 3, using eqs 4 and 5 to calculate $1/\Gamma_{diff}$.

systematic offset in the data. For the rest of the data, γ_{meas} is determined from the slope with the intercept fixed at zero.

As shown in eq 3, γ_{meas} includes a contribution from the gas-phase diffusion limitation on the uptake. The gas-phase diffusion contribution, Γ_{diff}, is calculated using eq 4 with Kn defined by eq 5 for the moving droplets in the droplet train flow reactor. The gas-phase diffusion coefficient, D_g, for 8−2 FTOH in He was estimated to be 0.135 atm cm^2 s^{-1} at 298 K using the Fuller et al. method described in Reid et al.[29] The temperature of the gas for the D_g calculation was assumed to be the average between the wall temperature (323 K) and the droplet surface temperature.[28] The temperature dependence of D_g was assumed to be $T^{1.7}$.[29] Because the experiments were done at a relatively low pressure of He, the gas-phase diffusion correction ($1/\Gamma_{diff}$) is small. For example, for the data in Figure 3, $1/\gamma_{meas} = 13.3$ and $1/\Gamma_{diff} = 1.1$, less than a 10% correction. The resulting $\gamma_0 = 0.082$.

To further test the effect of the gas-phase diffusion limitation on the uptake measurements, we performed experiments as a function of Kn by varying the total pressure in the flow tube and by using Ar as the carrier gas. The gas-phase diffusion coefficient for 8−2 FTOH in Ar was estimated to be 0.035 atm cm^2 s^{-1} at 298 K.[29] Figure 4 shows γ_{meas} as a function of Kn for FTOH uptake on 1-octanol droplets at 264 K. The line is calculated from eq 3, using eqs 4 and 5 to calculate $1/\Gamma_{diff}$, and provides a good fit to the experimental data with γ_0 as the only adjustable parameter. The asymptote at large Kn is γ_0, i.e., the uptake coefficient in the absence of gas-phase diffusion limitations.

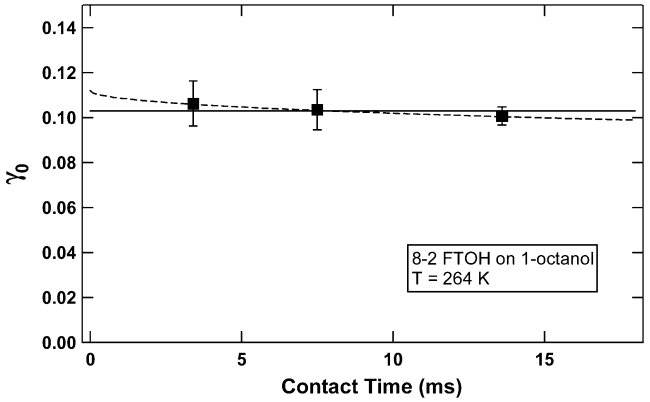

Figure 5. Uptake coefficient, γ_0, for 8−2 FTOH on 1-octanol as a function of gas−droplet contact time at 264 K (solid squares). The solid line shows the time-independent average value for $\gamma_0 = 0.103 \pm 0.009$. The dashed line shows a fit with eq 6, using eq 7 for Γ_{sat}.

Figure 5 shows γ_0 for 8−2 FTOH uptake on 1-octanol at 264 K as a function of contact time between the gas-phase species and the droplets. The contact time is varied by injecting the trace gas through the three different loop injectors located along the flow tube (see Figure 1). Within the error bars on the data points, γ_0 is independent of contact time as shown with the solid horizontal line. The lack of a time dependence indicates that $1/\Gamma_{sat}$ in eq 6 is small compared to $1/\alpha$ and the uptake is not limited by Henry's law solubility. In this case, $\gamma_0 = \alpha$.

We can estimate a lower limit for the Henry's law solubility by fitting the data with eq 6, using eq 7 for Γ_{sat}. The fit is shown with the dashed line in Figure 5 and gives a value of 13 M atm^{-1} cm s$^{-1/2}$ for the fit parameter $HD_l^{1/2}$. However, because the data points are fit equally well (within their error bars) with no time dependence (solid line), this is a lower limit for $HD_l^{1/2}$. In other words, if $HD_l^{1/2}$ were larger, the change in the data points with time would be greater than their error bars. We can estimate $D_l \approx 2 \times 10^{-7}$cm^2 s^{-1} for 8−2 FTOH in 1-octanol at 264 K using the Scheibel correlation method discussed in Reid et al.,[29] yielding a lower limit of 3×10^4 M atm^{-1} for the Henry's law solubility in 1-octanol.

No time dependence was observed for the uptake coefficient of 8−2 FTOH on 1-octanol at the five temperatures investigated in this study. The measured uptake coefficients, corrected for gas-phase diffusion, are therefore equal to the mass accommodation coefficients and are plotted as a function of temperature in Figure 6. The data are given in Table 1. The mass accommodation coefficient exhibits a negative temperature dependence similar to that observed previously for a wide variety of gas-phase molecules on aqueous and organic surfaces.[27,30−32]

The uptake of 8−2 FTOH on 1-octanol droplets was studied as a function of relative humidity at 264 K by adding water vapor to the flow tube carrier gas. Previous experiments have shown that the near-surface region of the droplets reaches equilibrium with the gas-phase water vapor within the transit time between the droplet generation chamber and the flow tube where uptake is measured.[27] No change in the uptake coefficient was observed even at 100% relative humidity.

Experiments were performed with different gas-phase densities of the 8−2 FTOH ranging from 2×10^{14} molecules cm^{-3} to 8×10^{14} molecules cm^{-3}. No change in the uptake coefficient was observed. We estimate that the number of 8−2 FTOH molecules deposited in the maximum gas−droplet contact time (20 ms), assuming the largest measured uptake coefficient, corresponds to between 2 and 8 monolayers of 8−2 FTOH for the lowest and highest gas-phase densities, respectively. Thus,

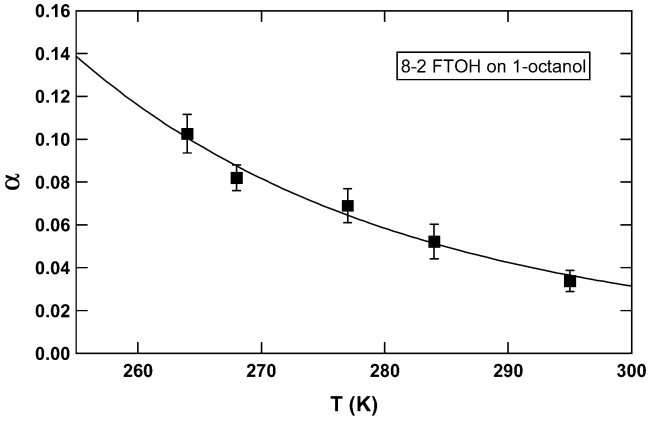

Figure 6. Mass accommodation coefficients, α, for 8−2 FTOH on 1-octanol as a function of temperature. The solid line is a fit to the data using eq 9 yielding $\Delta H_{obs} = -5.4 \pm 0.5$ kcal mol^{-1} and $\Delta S_{obs} = -24.7 \pm 1.9$ cal mol^{-1} K^{-1}.

TABLE 1: Mass Accommodation Coefficients for 8−2 FTOH on 1-octanol as a Function of Temperature (data in Figure 6)

temperature (K)	mass accommodation coefficient (α)
264	0.103 ± 0.009
268	0.082 ± 0.006
277	0.069 ± 0.008
284	0.052 ± 0.008
295	0.034 ± 0.005

the observation of no change in the uptake coefficient as a function of 8−2 FTOH gas-phase density probably rules out the contribution of surface reactions or the formation of surface complexes to the measured uptake coefficient.

Discussion

Mass Accommodation. As shown in Figure 6, the mass accommodation coefficients for 8−2 FTOH on 1-octanol have a negative temperature dependence. A negative temperature dependence for α was observed in previous uptake studies conducted with 40 hydrophilic gas-phase species on aqueous surfaces,[30] as well as for HCl on ethylene glycol surfaces[33] and HCl, acetic acid, γ-terpinene, *p*-cymene, and 2-methyl-2-hexanol on 1-octanol surfaces.[27,34] As discussed in our previous publications, the mass accommodation coefficient can be expressed as[31]

$$\frac{\alpha}{1-\alpha} = \frac{k_{sol}}{k_{des}} = \exp\left(\frac{-\Delta G_{obs}}{RT}\right) \qquad (9)$$

where k_{sol} and k_{des} are the rates of solvation and desorption for the trace gas molecules interacting with the liquid surface, respectively. The parameter $\Delta G_{obs} = \Delta H_{obs} - T\Delta S_{obs}$ is derived from the postulated free energy diagram for the vapor−liquid interface described in detail in Nathanson et al.[35] In this free energy scheme, the trace gas molecule can be in the gas phase, in a surface-bound state, or fully solvated in the liquid. There is no barrier between the gas-phase state of the molecule and the surface-bound state, while the barrier between the surface-bound state and the fully solvated state is related to the formation of critical clusters as described in the next paragraph.

Uptake studies on water surfaces led to the formulation of a classical nucleation critical-cluster model for mass accommodation.[31,35] In the nucleation critical-cluster model, the surface of the liquid is envisioned as a sharp but finite transition region

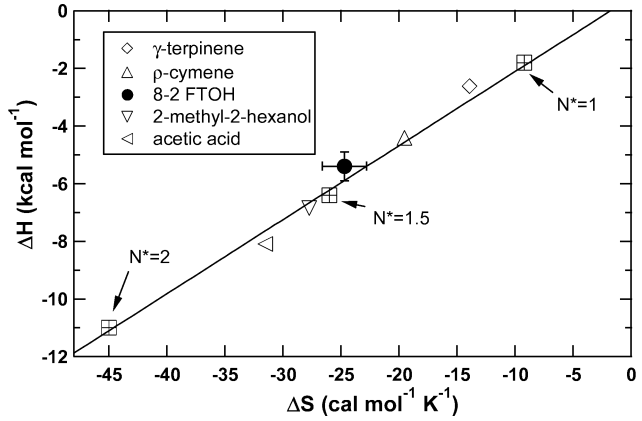

Figure 7. Experimental and calculated values of ΔH_{obs} and ΔS_{obs} for mass accommodation on 1-octanol surfaces. Symbols: (solid circle) 8−2 FTOH, this work; (open diamond) γ-terpinene; (open triangle) *p*-cymene; (open inverse triangle) 2-methyl-2-hexanol; (open wedge) acetic acid; (crossed square) calculated values of ΔH_{obs} and ΔS_{obs} for the indicated cluster size, from refs 27 and 34.

over several molecular diameters within which the density changes from liquid-phase to gas-phase values. This interface is a dynamic region where small clusters or aggregates of molecules constituting the liquid (in this case, 1-octanol) are continually forming, falling apart, and re-forming. The driving force, as described by classical nucleation theory, is such that clusters smaller than a critical size (N^*) fall apart, whereas clusters larger than the critical size serve as centers for further aggregation and grow in size until they merge into the adjacent bulk liquid. In this model, gas uptake proceeds via the growth of critical clusters. The incoming gas molecule, upon striking the surface, becomes a loosely bound surface species that participates in the surface nucleation process. If such a molecule becomes part of a critical-sized cluster, it will be incorporated into the bulk liquid via cluster growth. In this formulation, the critical cluster corresponds to the transition state between the surface-bound molecule and the fully solvated molecule. ΔG_{obs} corresponds to the difference in Gibbs free energy between the critical cluster and the gas phase, since there is no barrier between the gas-phase state and the surface-bound state.

The solid line in Figure 6 shows a fit to the mass accommodation data using eq 9, yielding $\Delta H_{obs} = -5.4 \pm 0.5$ kcal mol^{-1} and $\Delta S_{obs} = -24.7 \pm 1.9$ cal mol^{-1} K^{-1}. Figure 7 shows the value of ΔH_{obs} plotted versus ΔS_{obs} for mass accommodation of 8−2 FTOH on 1-octanol as determined in this study along with ΔH_{obs} and ΔS_{obs} values for several other organic molecules on 1-octanol.[27,34] ΔH_{obs} and ΔS_{obs} values for over 40 trace gas species on water surfaces lie on a straight line, a result that has been successfully explained with the critical-cluster nucleation theory.[31,35] The fact that the values of ΔH_{obs} and ΔS_{obs} for uptake on 1-octanol lie on a straight line suggests that the nucleation model of mass accommodation may also apply to uptake on 1-octanol surfaces. The crossed squares show calculated values of ΔH_{obs} and ΔS_{obs} for uptake on 1-octanol for various cluster sizes. (See ref 27 for the equations and details of the calculations.) The relative size of N^* represents the ease with which an incoming gas molecule enters into the nucleation or aggregation process with molecules of the liquid at the interface. Molecules with the ability to form strong bonds with 1-octanol form critical clusters more easily and thus exhibit a smaller N^*.

Atmospheric Implications. The small upper limit for the uptake of 8−2 FTOH on pure water indicates that, for atmospherically relevant conditions, the molecules are not likely to form significant surfactant layers on aqueous atmospheric droplets. Furthermore, because estimated Henry's law constants in water are small for the FTOHs of interest at atmospheric temperatures,[36] the uptake of FTOHs on or into the aqueous component of cloud/fog droplets or aqueous aerosol particles is not likely to be an important atmospheric sink for these compounds.

In contrast, the larger uptake coefficient measured for 1-octanol surfaces indicates that FTOH partitioning to organic-containing cloud/fog droplets and aerosol particles may be an effective loss mechanism under some atmospheric conditions. Cloud/fog droplets may have significant amounts of organic materials that are accessible to low vapor pressure gaseous molecules, as evidenced by the measurements of Glotfelty et al.[15,16] that found relatively insoluble organic pesticides and plasticizers in cloud droplets at concentrations tens to thousands of times higher than their water Henry's law solubility values would predict. This will most likely occur if the fog droplets contain an organic phase that can host the excess organic species.

It is now widely recognized that organic material originating from both natural and anthropogenic sources makes up a large fraction of much of the fine atmospheric aerosol.[37,38] The possibility that organic molecules adsorbed on the surface of aqueous aerosol particles may influence heterogeneous chemical processes has also been recognized.[39,40] Recent measurements indicated that even continental sulfate aerosol particles may have significant coatings of organic surfactants.[41] Furthermore, by using a novel aerosol mass spectrometer developed and used in our laboratories, we have shown that the organic fraction typically constitutes between $^1/_4$ and $^2/_3$ of the nonrefractory (i.e., not graphitic soot or mineral matter) mass fractions of aerosol particles with aerodynamic diameters below 1 μm.[42,43] This is important because these "accumulation mode" particles usually dominate the aerosol particle surface area and thus control atmospheric trace gas aerosol particle heterogeneous processes.

The impact of organic material associated with cloud/fog droplets and aerosol particles on the atmospheric lifetimes of airborne FTOHs will vary with the levels of organic material found in the atmosphere. Atmospheric models do not currently quantify accurately either the amounts or the chemical speciation of aerosol or fog/cloud droplet organic materials or capture their complex heterogeneous kinetics.[44] While the observed uptake of 8−2 FTOH on 1-octanol strongly suggests that uptake by condensed-phase airborne organic matter will reduce the atmospheric lifetimes of FTOHs, especially in regions with high anthropogenic or biogenic organic emissions, the quantitative evaluation of this effect will require more sophisticated heterogeneous chemistry models than those currently available. Since the distribution of organic aerosol varies strongly with location and time of year, and the degree to which uptake on 1-octanol surfaces represents the uptake to typical organic aerosol particle surfaces is unknown, the potential effect of heterogeneous uptake of FTOHs on organic aerosol particles and the organic component of cloud/fog droplets represents a significant uncertainty in our current knowledge of FTOH atmospheric fate.

Acknowledgment. The authors dedicate this paper to David Golden to honor his pioneering role in the application of the Knudsen cell technique to the study of trace gas uptake kinetics on liquid surfaces representative of atmospheric aerosol particles, and to recognize his many other contributions to physical chemistry and its applications. L. R. Williams acknowledges and greatly appreciates mentoring by David Golden in the early stages of her career. Funding for this work was provided by E.I. du Pont de Nemours and Company, contract #LMD-623169.

Valuable technical input from R. L. Waterland and R. C. Buck of du Pont is acknowledged, and their interest in and support of these studies is appreciated.

Supporting Information Available: Values for the data points in Figures 2−5 and 7. This material is available free of charge via the Internet at http://pubs.acs.org.

References and Notes

(1) Rao, N. S.; Baker, B. E. In *Organofluorine Chemistry. Principles and Commercial Applications*; Banks, R. E., Smart, B. E., Tatlow, J. C., Eds.; Plenum Press: New York, 1994; pp 321−336.

(2) Kissa, E. *Fluorinated Surfactants and Repellents*; Marcel Dekker: New York, 2001; Vol. 97.

(3) Krusic, P. J.; Marchione, A. A.; Davidson, F.; Kaiser, M. A.; Kao, C.-P. C.; Richardson, R. E.; Botelho, M.; Waterland, R. L.; Buck, R. C. *J. Phys. Chem. A* **2005**, *109*, 6232−6241.

(4) Kaiser, M. A.; Cobranchi, D. P.; Kao, C.-P. C.; Krusic, P. J.; Marchione, A. A.; Buck, R. C. *J. Chem. Eng. Data* **2004**, *49*, 912−916.

(5) Buck, R. C. Personal communication, 2005.

(6) Stock, N. L.; Lau, F. K.; Ellis, D. A.; Martin, J. W.; Muir, D. C. G.; Mabury, S. A. *Environ. Sci. Technol.* **2004**, *38*, 991−996.

(7) Martin, J. W.; Muir, D. C. G.; Moody, C. A.; Ellis, D. A.; Kwan, W. C.; Solomon, K. R.; Maybury, S. A. *Anal. Chem.* **2002**, *74*, 584−590.

(8) Ellis, D. A.; Martin, J. W.; De Silva, A. O.; Mabury, S. A.; Hurley, M. D.; Sulbaek Andersen, M. P.; Wallington, T. J. *Environ. Sci. Technol.* **2004**, *37*, 3316−3321.

(9) Ellis, D. A.; Martin, J. W.; Maybury, S. A.; Hurley, M. D.; Anderson, M. P.; Wallington, T. J. *Environ. Sci. Technol.* **2003**, *37*, 3816−3820.

(10) Hurley, M. D.; Ball, J. C.; Wallington, T. J.; Sulbaek Andersen, M. P.; Ellis, D. A.; Martin, J. W.; Mabury, S. A. *J. Phys. Chem. A* **2004**, *108*, 5653−5642.

(11) Ellis, D. A.; Martin, J. W.; Maybury, S. A.; Hurley, M. D.; Anderson, M. P.; Wallington, T. J. *Environ. Sci. Technol.* **2003**, *37*, 3816−3820.

(12) Sulbaek Andersen, M. P.; Nielsen, O. J.; Hurley, M. D.; Ball, J. C.; Wallington, T. J.; Ellis, D. A.; Martin, J. W.; Mabury, S. A. *J. Phys. Chem. A* **2005**, *109*, 1849−1856.

(13) Waterland, R. L.; Hurley, M. D.; Misner, J. A.; Wallington, T. J.; Melo, S. M. L.; Strong, K.; Dumoulin, R.; Castera, L.; Stock, N. L.; Mabury, S. A. *J. Fluorine Chem.* **2005**, *126*, 1288−1296.

(14) Chen, L.; Takenaka, N.; Bandow, H.; Maeda, Y. *Atmos. Environ.* **2003**, *37*, 4817−4822.

(15) Glotfelty, D. E.; Majewski, M. S.; Seiber, J. N. *Environ. Sci. Technol.* **1990**, *24*, 353−357.

(16) Glotfelty, D. E.; Seiber, M. S. J. N.; Liljedahl, L. A. *Nature (London)* **1987**, *325*, 602−605.

(17) Cousins, I. T.; Mackay, D. *Environ. Sci. Technol.* **2001**, *35*, 643−647.

(18) Falconer, R. L.; Harner, T. *Atmos. Environ.* **2000**, *34*, 4043−4046.

(19) Jayne, J. T.; Duan, S. X.; Davidovits, P.; Worsnop, D. R.; Zahniser, M. S.; Kolb, C. E. *J. Phys. Chem.* **1991**, *95*, 6329−6336.

(20) Fuchs, N. A.; Sutugin, A. G. *Highly Dispersed Aerosols*; Ann Arbor Science Publishers: Newton, MA, 1970.

(21) Widmann, J. F.; Davis, E. J. *J. Aerosol Sci.* **1997**, *28*, 87−106.

(22) Seinfeld, J. H.; Pandis, S. N. *Atmospheric Chemistry and Physics: From Air Pollution to Climate Change*; John Wiley and Sons: New York, 1998.

(23) Hanson, D. R.; Ravishankara, A. R.; Lovejoy, E. R. *J. Geophys. Res.* **1996**, *101*, 9063−9069.

(24) Worsnop, D. R.; Shi, Q.; Jayne, J. T.; Kolb, C. E.; Swartz, E.; Davidovits, P. *J. Aerosol Sci.* **2001**, *32*, 877−891.

(25) Morita, A.; Sugiyama, M.; Koda, S. *J. Phys. Chem. A* **2003**, *107*, 1749−1759.

(26) Shi, Q.; Davidovits, P.; Jayne, J. T.; Worsnop, D. R.; Kolb, C. E. *J. Phys. Chem. A* **1999**, *103*, 8812−8823.

(27) Zhang, H. Z.; Li, Y. Q.; Xia, J.-R.; Davidovits, P.; Williams, L. R.; Jayne, J. T.; Kolb, C. E.; Worsnop, D. R. *J. Phys. Chem. A* **2003**, *107*, 6388−6397.

(28) Worsnop, D. R.; Zahniser, M. S.; Kolb, C. E.; Gardner, J. A.; Watson, L. R.; Doren, J. M. V.; Jayne, J. T.; Davidovits, P. *J. Phys. Chem.* **1989**, *93*, 1159−1172.

(29) Reid, R. C.; Prausnitz, J. M.; Poling, B. E. *The Properties of Gases and Liquids*; McGraw-Hill Book Co.: New York, 1987.

(30) Kolb, C. E.; Davidovits, P.; Jayne, J. T.; Shi, Q.; Worsnop, D. R. *Prog. React. Kinet. Mech.* **2002**, *27*, 1−46.

(31) Davidovits, P.; Jayne, J. T.; Duan, S. X.; Worsnop, D. R.; Zahniser, M. S.; Kolb, C. E. *J. Phys. Chem.* **1991**, *95*, 6337−6340.

(32) Li, Y. Q.; Zhang, H. Z.; Davidovits, P.; Jayne, J. T.; Kolb, C. E.; Worsnop, D. R. *J. Phys. Chem. A* **2002**, *106*, 1220−1227.

(33) Li, Y. Q.; Davidovits, P.; Shi, Q.; Jayne, J. T.; Kolb, C. E.; Worsnop, D. R. *J. Phys. Chem. A* **2001**, *105*, 10627−10634.

(34) Zhang, H. Z.; Li, Y. Q.; Xia, J.-R.; Davidovits, P.; Williams, L. R.; Jayne, J. T.; Kolb, C. E.; Worsnop, D. R. *J. Phys. Chem. A* **2003**, *107*, 6398−6407.

(35) Nathanson, G. M.; Davidovits, P.; Worsnop, D. R.; Kolb, C. E. *J. Phys. Chem.* **1996**, *100*, 13007−13020.

(36) Stock, N. L.; Ellis, D. A.; Deleebeeck, L.; Muir, D. C. G.; Maybury, S. A. *Environ. Sci. Technol.* **2004**, *38*, 1693−1699.

(37) Jacobson, M. C.; Hansson, K. J.; Charlson, R. J. *Rev. Geophys.* **2000**, *38*, 267−294.

(38) Seinfeld, J. H.; Pankow, J. F. *Annu. Rev. Phys. Chem.* **2003**, *54*, 121−140.

(39) Gill, P. S.; Graedel, T. E.; Weschler, C. J. *Rev. Geophys.* **1983**, *21*, 903.

(40) Ellison, G. B.; Tuck, A. F.; Vaida, V. *J. Geophys. Res.* **1999**, *104*, 11633.

(41) Tervahattu, H.; Juhanoja, J.; Vaida, V.; Tuck, A. F.; Niemi, J. V.; Kupiainen, K.; Kulmala, M.; Vehkamäki, J. *J. Geophys. Res.* **2005**, *110*, D06207.

(42) Jiménez, J. L.; Jayne, J. T.; Shi, Q.; Kolb, C. E.; Worsnop, D. R.; Yourshaw, I.; Seinfeld, J. H.; Flagan, R. C.; Zhang, X.; Smith, K. A.; Morris, J.; Davidovits, P. *J. Geophys Res.* **2003**, *108*, 8425.

(43) Drewnick, F.; Schwab, J. J.; Jayne, J. T.; Canagaratna, M.; Worsnop, D. R.; Demerjian, K. L. *Aerosol Sci. Technol.* **2004**, *38*, 92−103.

(44) Rudich, Y. *Chem. Rev.* **2003**, *103*, 5097−5124.